



Evidence of Hubble Flow-like Motion of Young Stellar Populations away from the Perseus Arm

Carlos G. Román-Zúñiga^{1,2} , Alexandre Roman-Lopes^{2,3} , Mauricio Tapia^{1,2} ,
Jesús Hernández¹ , and Valeria Ramírez-Preciado¹

¹ Instituto de Astronomía, Universidad Nacional Autónoma de México, Unidad Académica en Ensenada, Ensenada 22860 Mexico; croman@astro.unam.mx

² Programa de Estancias de Investigación (PREI), DGAPA-UNAM, Mexico

³ Departamento de Física y Astronomía, Universidad La Serena, La Serena, Chile

Received 2018 August 19; revised 2018 December 12; accepted 2018 December 26; published 2019 January 22

Abstract

In this Letter we present evidence of the coherent outward motion of a sample of young stars ($t < 30$ Myr) in the Perseus Arm, whose apparent origin is located in the vicinity of the W3/W4/W5 complex. Using astrometric and photometric data from the *Gaia* Data Release 2 catalog of an 8° radius field centered near W4, we selected a sample of young intermediate- to high-mass star candidates. The sample is limited to sources with parallax uncertainties below 20% and Bayesian distance estimates within 1800 and 3100 pc. The selection includes embedded stellar populations as well as young open clusters. Projected velocities derived from perspective-corrected proper motions clearly suggest that the young star population emerged from the Perseus Arm, with a possible convergence zone near W3/W4/W5 region, tracing a front that expands away at a rate of about $15 \text{ km s}^{-1} \text{ kpc}^{-1}$.

Key words: Galaxy: kinematics and dynamics – open clusters and associations: general – stars: kinematics and dynamics – stars: massive

1. Introduction

Star clusters are formed within giant molecular clouds (GMCs) with a large diversity, likely related to the early organization of the clouds and environmental factors (Lada & Lada 2003; Longmore et al. 2014). In a recent review, Gouliermis (2018, and references therein) discussed the case of gravitationally unbound young stellar systems, representing GMC complex-scaled multiplex associations that may be considered to be the open end of an intricate, hierarchical process that scales down to the formation of compact, bound clusters. In that scenario, large GMC complexes may produce a large number of star clusters born with a variety of energy distributions (Blaauw 1964) that, in most cases: (a) expand and disperse, (b) can be traced through their massive (OB) members, and (c) may contain crucial information about their formation process. In general, the expansion and dispersal of young star systems may be related to complex dynamical interactions between clusters and sub-clusters during their formation process, and also to the rapid removal of gas due to massive star winds and more violent events like Wolf-Rayet outbursts or supernova explosions. The current availability of precise astrometric parameters (distances, proper motions) from the *Gaia* satellite Data Release 2 (DR2; see Gaia Collaboration et al. 2016, 2018) allows the exploration of star kinematics in this context, and it has provided evidence of coherent motion and expansion of stellar populations in certain stellar systems, from star-forming complexes (e.g., Kounkel et al. 2018; Kuhn et al. 2019) to more evolved young cluster associations (e.g., Wright & Mamajek 2018) and OB associations with driven expansion (e.g., Cantat-Gaudin et al. 2019).

The goal of this Letter is to report a discovery about the global picture of star cluster evolution in a region of the Perseus Arm (hereafter PsAm), around the W3/W4/W5 complex (hereafter W345). W345, located on the Galactic plane, is a well-studied massive star-forming region, containing two giant

H II regions (W4 and W5), a massive molecular ridge with active formation (W3), and several embedded star clusters (e.g., Carpenter et al. 2000; Koenig et al. 2008; Román-Zúñiga et al. 2015; Jose et al. 2016; Sung et al. 2017) possibly hosting a large number of OB stars. Around W345, this region of the PsAm hosts several OB associations like Per OB1, which contains the open clusters NGC 884 and 869, and the Cassiopeia OB8, which includes the cluster NGC 663. Here we show that a sample of intermediate- to high-mass young stars in W345 and nearby associations traces what looks like a coherent expanding front of young ($t < 30$ Myr) stars and clusters, likely born at the PsAm close to the W345 region.

2. Data Sample Selection and Analysis

Our main goal is to study the kinematics of intermediate to massive (OB) stars as tracers of the young stellar population in W345 and its surroundings. Using the *Gaia* Table Access Protocol (TAP) services and catalog extraction tool at Astronomisches Rechen-Institut,⁴ we retrieved a catalog comprising all DR2 entries within an 8° -radius cone centered on the W345 complex at $(\alpha, \delta) = (40^\circ, 61^\circ)$.⁵ The catalog contains a full set of photometric (G , B_p , and R_p magnitudes) and astrometric (proper motions, μ_p , parallaxes, ϖ and parallax errors, σ_ϖ) parameters. This cone extends roughly from 250 to 420 pc (depending on distance) in each direction from the W345 complex, covering the projected width of the PsAm and providing a good sampling of the populations formed at GMC complexes in the region.

The TAP tool also provides distance estimates for each star by using a Galactic stellar density model prior that varies with each position (l, b) (Bailer-Jones et al. 2018) and provides confidence intervals, defined by lower and upper limits, d_{low}

⁴ <http://gaia.ari.uni-heidelberg.de/>

⁵ We confirmed that a larger opening does not alter our results significantly.

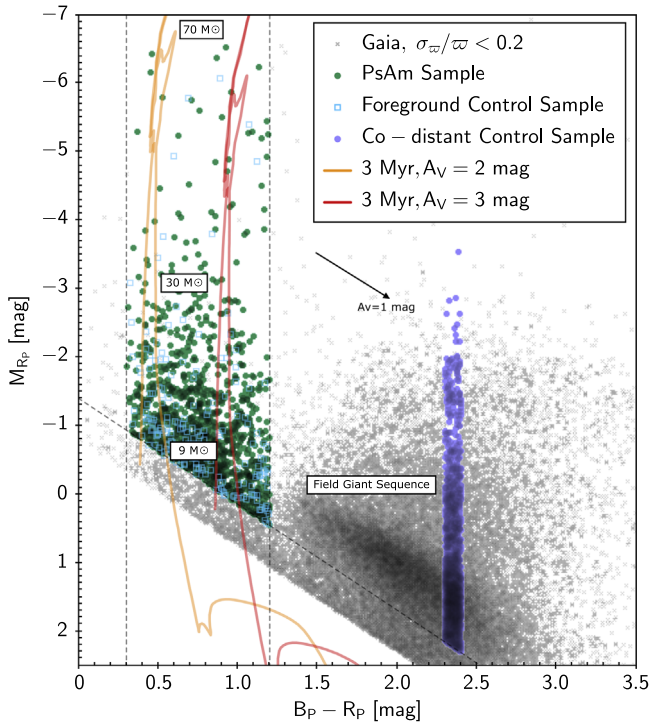


Figure 1. *Gaia* color-absolute magnitude diagram showing the selection of a sample containing OB stars. Gray symbols are *Gaia* sources in the main catalog with parallax errors under 20%. Green symbols indicate the PsAm sample. Yellow and cyan symbols show the control samples. The color/brightness constraints (Section 2) are indicated with dotted lines. The solid color lines are 3 Myr isochrones from the PARSEC 1.2 s models (Bressan et al. 2012; Tang et al. 2014).

and d_{high} . We extracted sources within $1.8 < (d/\text{kpc}) < 3.1$, which we define as a “full” sample expected to contain sources across the entire girth of the PsAm. We limited the sample to sources with $\sigma_{\varpi}/\varpi < 0.2$ parallax accuracy⁶ and contained within a distance range defined by $(d_{\text{high}} - d_{\text{low}}) < 1.2d + 20$. As shown in Figure 1, using the M_{R_p} versus $B_p - R_p$ *Gaia* color-absolute magnitude diagram, we selected a locus containing sources brighter than $1.547 \times (B_p - R_p) - 1.2$ (the slope follows the reddening vector using the extinction coefficients from Evans et al. 2018) and colors within $0.3 < B_p - R_p < 1.2$ mag. This locus minimizes contamination from field giant and dwarf stars, and is expected to contain mostly bright intermediate to massive members of young stellar groups with average extinctions within $A_V = 1$ and 3 mag. We estimate around 10% of contamination in this sample due to field stars with anomalous colors, with a distribution affected by patchy extinction. Finally, we also restricted the projected raw velocity moduli to $\sqrt{v_l^2 + v_b^2} = |v| < 60 \text{ km s}^{-1}$. The total number of sources in this restricted PsAm sample is 1100.

From the distances and proper motions, we calculated projected velocities over the plane of the sky on galactic coordinates as $v_{l,b} = 4.74d\mu_{l,b}$, where μ_l and μ_b are directly transformed from the μ_{α} and μ_{δ} values provided in the DR2.⁷ The angular size of the region of study is quite large, thus requiring a correction by perspective expansion/contraction (Brown et al. 1997) to take into account the effect of the motion

perpendicular to the plane of the sky. We followed the prescription of Gaia Collaboration et al. (2018) by first defining an expansion center at $(l, b) = (137^\circ.8, 1^\circ.3)$ (see also Section 3), located near the young cluster IC 1805 in W4. We then derived a new set of orthographically projected positions (x_p, y_p) , and proper motions (μ_{x_p}, μ_{y_p}) , relative to that center. Assuming that rotation and inclination effects in the PsAm are negligible, the variation of the projected proper motions as a function of the projected positions, to first order, will only keep the bulk motion component perpendicular to the line of sight: $\partial\mu_x/\partial x \approx \partial\mu_y/\partial y \approx -v_z$. This way, a linear fit to either of the μ_{x_p} versus x_p or μ_{y_p} versus y_p plots provides, to first order, a direct estimate of the required perspective correction. In our case, the resultant correction is $c_{\mu_{l,b}} \approx 5.4(x_p, y_p) \text{ mas yr}^{-1}$, applied to the orthographically projected positions, which we finally subtracted from the DR2 proper motions. This accounts for the required perspective correction by the unknown line of sight motion of each star.

Now, it is important to consider that without radial velocity data, it is impossible to determine whether the observed expansion is due to purely perspective or purely physical effects. In order to quantify this, we followed Blaauw (1964) and Wright & Mamajek (2018; their Equations (3) and (4)): for a system in linear expansion with an age τ , it is possible to predict the required radial velocities as the sum of the star velocities measured from the system barycenter and an expansion age term⁸ $\kappa d = (1.0227\tau)^{-1}d$. Using a Monte Carlo routine, we found that for stars with $1 < \tau < 50$ Myr (see Section 3), the expected distribution for κd has a well-defined peak around 100 km s^{-1} . We are able to reproduce well that distribution by providing our sample with radial velocity values in the range $-15 < v_R < -65 \text{ km s}^{-1}$, i.e., around the local standard of rest velocity for the W345 clouds (e.g., Heyer et al. 1998; Bieging & Peters 2011). We failed to emulate the κd distribution when we increased the radial velocity interval to over 100 km s^{-1} . Radial velocity corrections so large are physically unreasonable as a solely perspective effect. Therefore, we can safely consider our sample to present a physical expansion.

Finally, we applied the same constraints to two control samples within the same cone: one (foreground control sample) limited to sources with distances $d < 1300 \text{ pc}$ (i.e., unrelated to the PsAm) and a second one (co-distant control sample), containing stars in the same distance range but sampling an older population dominated by field giants within $2.3 < (B_p - R_p) < 2.4$. The resultant samples contain 193 and 2468 stars, respectively. The purpose of these control samples is to apply a similar analysis to them, and assure that the observed behavior (see Section 3) of the young massive candidates in the PsAm is not a data-related effect (e.g., present in the whole *Gaia* DR2 sample in this direction of the Galaxy).

3. Results

In Figure 2 we show the perspective-corrected projected velocities $v_{l,pc}$, $v_{b,pc}$ (scaled to units of 500 pc/Myr) for the *Gaia* DR2 stars present in the full distance sample, over a map that traces star-forming regions, as well as the distribution of molecular and neutral gas near W345, using $12 \mu\text{m}$ emission as well as H I and CO integrated intensity. As a visualization aid, we use an orientation parameter by calculating the dot product

⁶ A tighter constraint of $\sigma_{\varpi}/\varpi \leq 0.1$ does not significantly alter our results.

⁷ All proper motions and velocities are expressed units of mas yr^{-1} and km s^{-1} , respectively.

⁸ Plus a redshift/blueshift correction, which is negligible in our case.

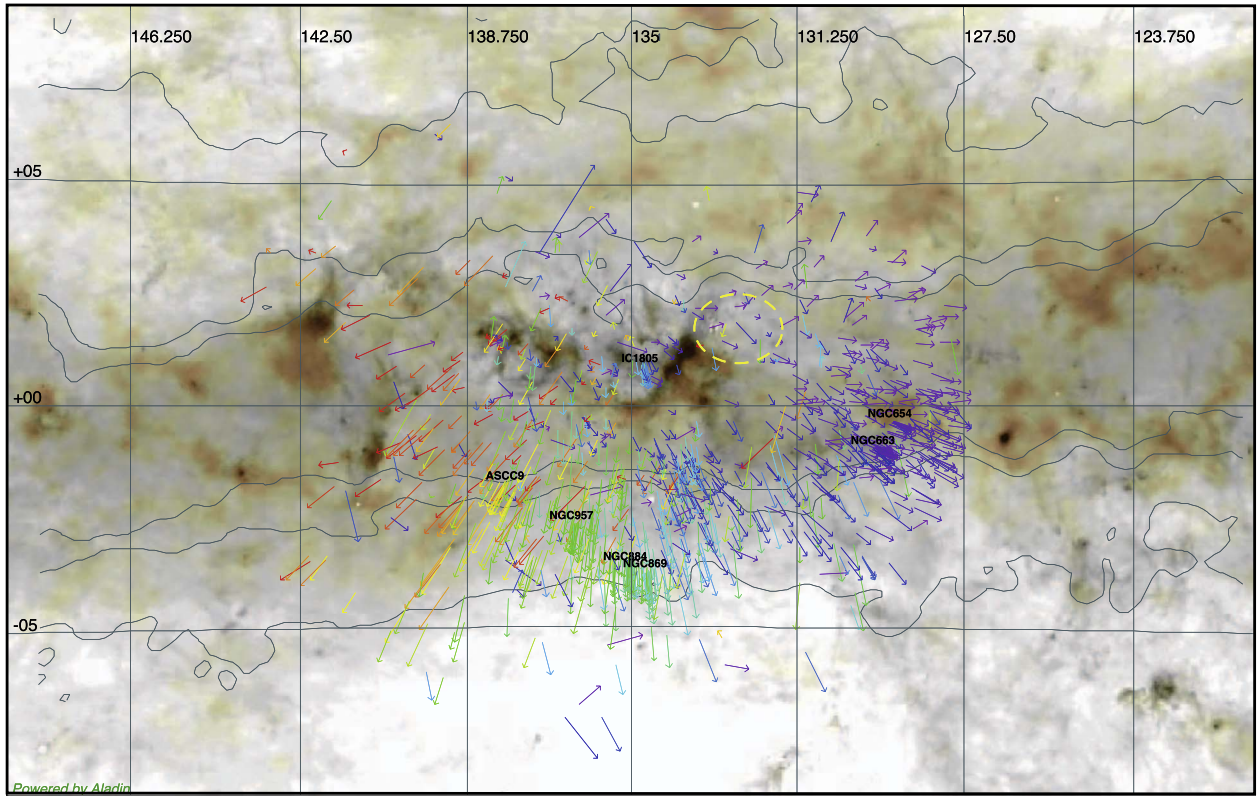


Figure 2. Perspective-corrected projected velocity map for the full sample, in Galactic coordinates. The background in grayscale is a *WISE* WSSA $12\ \mu\text{m}$ infrared emission map. The orange-red hue indicates regions of strong CO emission from the composite survey of Dame et al. (2001). Notice that most of the CO emission above $b \sim 3^\circ$ corresponds to clouds in the Local Arm, not Perseus. The contours indicate H I column density (EBHIS+GASS surveys HI4PI Collaboration et al. 2016) in levels of $50\text{--}200\ \text{cm}^{-2}/\text{healpix}$. The arrows indicate projected velocities scaled to units of $500\ \text{pc}\ \text{Myr}^{-1}$ for visualization purposes. The colors of the arrows in this map are parametrized by $\cos\theta$. The region delimited by the yellow dashed line indicates the approximate extension of the HB-3 supernova remnant near W3. Young open clusters in the region are indicated with labels.

between the corrected projected velocity, $v_{l,\text{pc}}$, and a purely horizontal unit proper motion vector $v_{l,\text{pc}} = (1, 0)$, as $\cos\theta = v_{l,\text{pc}}/|v_{l,\text{pc}}|$. The most striking feature in this map is the high degree of coherence in the orientation of the vectors on the plane of the sky, pointing away from W345, increasing in magnitude with distance. On the other hand, the selected sample covers the current star-forming regions in W345, and highlights several source overdensities that correspond to well-known young open clusters (see also Figure 4). For instance, the overdensity near $(l, b) = (135, -0.4)$ corresponds to NGC 884 and NGC 869 in the Per OB1 association, also known as $h + \chi$ Persei (10–13 Myr old, $d = 2.5 \pm 0.2$ kpc Currie et al. 2010). We can also distinguish two clear groups in the westernmost edge corresponding to NGC 663 and NGC 654 of the Cas OB8 association (20 Myr old, $d = 2.4 \pm 0.2$ kpc Tapia et al. 1991; Pandey et al. 2005).⁹ Another very important feature that emerges from Figure 2 is that for the perspective-corrected motions for the control sample, we cannot identify any grouping and the vectors present a net null trend, with the majority of the sources moving in directions parallel to the Galactic disk. This confirms that the above effect is actually associated to the PsAm population.

In Figure 3 we show the perspective-corrected proper motions (a dot-vector plot) for the full and the control sample. We clearly see that while the PsAm stars form a tight, well-defined structure with several overdensities (that correspond

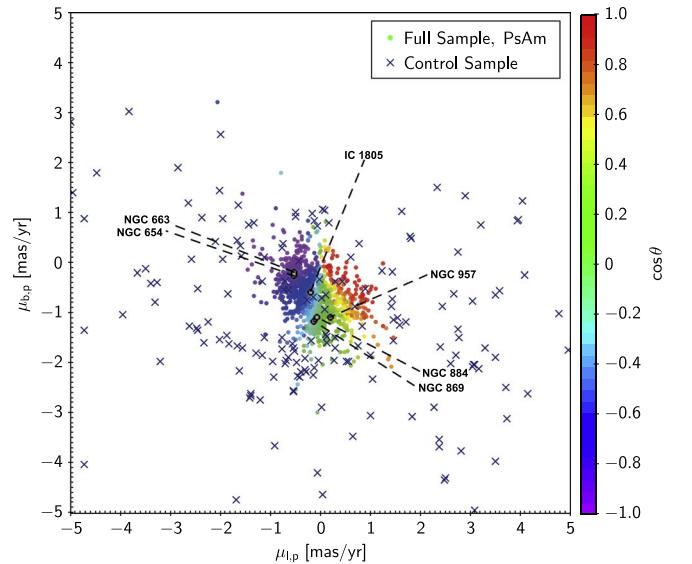


Figure 3. Perspective-corrected proper motions for the full sample (color parametrized by $\cos\theta$) and the control sample (blue X symbols). The average values for cluster member candidates are indicated with the black dots and labels.

well with the larger groups), the control sample sources appear significantly dispersed, indicating very little or no coherence. In the first panel of the Figure set 4 we show the perspective-corrected, projected velocity modulus $|v|$ as a function of the projected distance, d_{cen} , from a convergence area centered at

⁹ Photometric distances. The DR2 parallaxes suggest larger distances, near 3 kpc, for these two clusters.

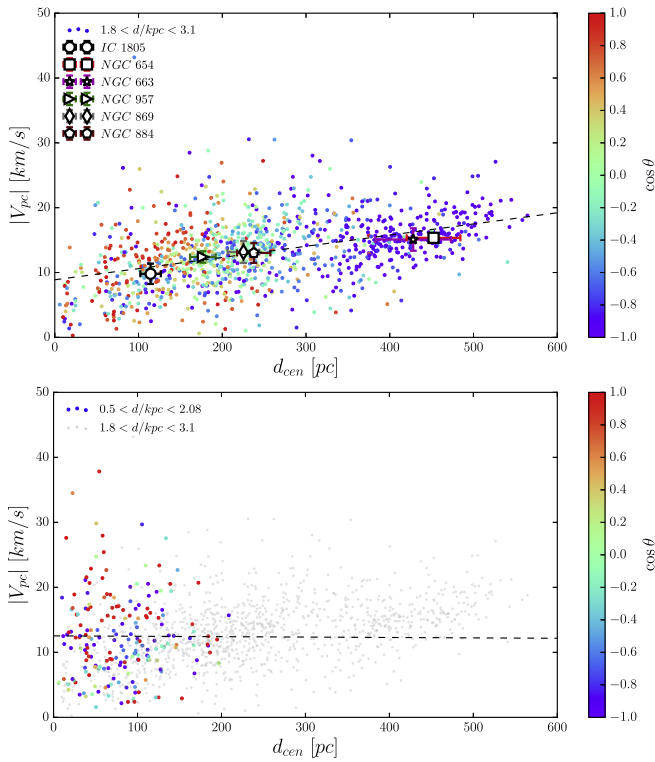


Figure 4. Perspective-corrected projected velocity moduli $|v|$ as a function of projected distance, d_{cen} from an estimated convergence point ($l = 137.8$, $b = 1.3$). The top and bottom panels show the result for the PsAm and the control sample, respectively. The positions of known young open clusters are shown as large polygon-shaped symbols with error bars.

$(l, b) = (137.8, 1.3)$, which was estimated by projecting backwards the v_l, v_b vectors of candidate members of known open clusters, (defined as sources within a small vicinity around published centers and distances and limited to $\sigma_w/\varpi < 0.1$). We can see how the corrected velocity moduli for most of the sources are in the range of 10–20 km s^{-1} , which is significantly larger than the typical expansion velocities for unbound groups in other systems (e.g., Cantat-Gaudin et al. 2019; Kuhn et al. 2019; Wright & Mamajek 2018). It is clear that the young stellar population is actually expanding away from the Galactic plane: a linear fit to the data suggests a (projected) Hubble-type expansion of about $15.4 \text{ km s}^{-1} \text{ kpc}^{-1}$. The additional panel of the Figure 4 shows the equivalent plot for the control sample, where we confirm a null expansion trend, with a correlation coefficient near zero. The results for the co-distant control sample are equivalent, with a null expansion trend and little or no coherence in the dot-vector plot.

4. Discussion and Summary

The analysis of the *Gaia* DR2 data described above reveals a scenario where young stellar populations are moving away from a location in the PsAm. Tracing back the (v_l, v_b) vectors points to a convergent region near the W345 complex that currently hosts embedded populations as young as 1.5 Myr (likely the most recent star formation episode in the region). A satisfactory explanation of the effect and its consequences for currently accepted Galactic star formation scenarios is beyond the scope of this Letter, as more precise data would be required.

For instance, the *Gaia* DR2 parallaxes provide distances that are still uncertain in the 10^2 pc scale for the PsAm, impeding an accurate analysis of the distribution of young stellar populations within this part of the Arm. Also, the lack of radial velocity measurements for most of the stars in our sample prevents a full six-dimensional position–velocity analysis at this Galactic region. From the observed expanding motion and the available theories in the literature, we propose three possible scenarios.

1. The presence of the HB-3 supernova (SN) remnant near W3, along with the presence of tens of OB stars in the W345 complex (see the top panel Figure 2), suggest that SN explosions could be one possible driving mechanism in the region, which could transfer the mechanical energy to the cluster-gas systems. Indeed, it is known that a single SN can imprint momentum of the order of $10^5 M_\odot \text{ km s}^{-1}$ (Kim & Ostriker 2015), providing up to 10^{50} erg in 10 Myr (Thornton et al. 1998). Super-bubble-type expansions via SN often pierce and surpass the disk, depending on the homogeneity of the local medium (Mac Low et al. 1989). Also, most of the mechanical energy from SN events and massive star winds is carried by ionizing radiation, which could provide impulse for the stellar system expansion. *Gaia* DR2 data could provide evidence of a champagne-flow-type expansion of gas layers (Tenorio-Tagle 1979), with the stars moving *along with the gas*.
2. Recently, Tchernyshyov et al. (2018) presented detailed gas velocity maps and compared them to the Stationary Density Wave model of the Milky Way spiral structure (Lin & Shu 1964), particularly near the PsAm. The study suggests that a spiral arm can be fed from one side by diffuse gas causing a net outward flow toward its trailing edge. The main effect is a concentration of the dense gas where flows converge, and a dissipation of those centers after star formation, forming a divergence of the velocity field. This mechanism can provide a direct explanation of the observed effect in our sample. Moreover, if gas and stars are expelled away from the arm, aided by this mechanism, then we should expect a net torque in the arm. If this is true, our study presents actual evidence of the action of spiral density waves near the co-rotation radius in the PsAm.
3. Another possibility is that all the groups that we are considering are all part of a much larger association of clusters that is expanding away as a massive unbound young stellar system with an age spread of about 30 Myr (considering the estimated ages of the older clusters in the sample). The driving mechanisms behind the expansion could be directly related to the star formation process, along with gas dispersal and the dynamic evolution of the system, similar to what is observed in star-forming complexes like Orion, Vela OB2, or Scorpio–Centaurus. However, it would be necessary to determine how to adjust such proposed scenarios to the spiral arm width scale that we report in this Letter.

While eloquent, our analysis is just a starting point. Future work requires us to search for this effect in other massive star-forming regions in the nearby spiral arms. Large-scale spectroscopy projects like APOGEE-2 will provide precise radial velocity information at least near W345 (see Zasowski et al. 2017), allowing for a more complete vision, specially as the precision of *Gaia* data increases in the following releases.

We thank an anonymous referee for providing crucial comments and suggestions that greatly improved the manuscript. We thank Luis Aguilar for fruitful discussions and advice. V.R.P. acknowledges support from a CONACYT/UNAM scholarship. C.R.Z., V.R.P., M.T., and J.H. acknowledge support from UNAM-DGAPA-PAPIIT grants IN108117, IN104316, and IA103017, Mexico. A.R.L. acknowledges support from program FONDECYT 1170476, Chile and a PREI-DGAPA-UNAM academic exchange scholarship.

This work has made use of data from the European Space Agency (ESA) mission *Gaia* (<https://www.cosmos.esa.int/gaia>), processed by the *Gaia* Data Processing and Analysis Consortium (DPAC, <https://www.cosmos.esa.int/web/gaia/dpac/consortium>). Funding for the DPAC is provided by the institutions participating in the *Gaia* Multilateral Agreement.

Facility: *Gaia*.

Software: Aladin (Bonnarel et al. 2000), TOPCAT (Taylor 2005), AstroPy (Astropy Collaboration et al. 2013, 2018).

ORCID iDs

Carlos G. Román-Zúñiga  <https://orcid.org/0000-0001-8600-4798>

Alexandre Roman-Lopes  <https://orcid.org/0000-0002-1379-4204>

Mauricio Tapia  <https://orcid.org/0000-0002-0506-9854>

Jesús Hernández  <https://orcid.org/0000-0001-9797-5661>

Valeria Ramírez-Preciado  <https://orcid.org/0000-0002-4013-2716>

References

Astropy Collaboration, Price-Whelan, A. M., Sipőcz, B. M., et al. 2018, *AJ*, 156, 123
 Astropy Collaboration, Robitaille, T. P., Tollerud, E. J., et al. 2013, *A&A*, 558, A33

Bailer-Jones, C. A. L., Rybizki, J., Fouesneau, M., Mantelet, G., & Andrae, R. 2018, *AJ*, 156, 58
 Biegging, J. H., & Peters, W. L. 2011, *ApJS*, 196, 18
 Blaauw, A. 1964, *ARA&A*, 2, 213
 Bonnarel, F., Fernique, P., Bienaymé, O., et al. 2000, *A&AS*, 143, 33
 Bressan, A., Marigo, P., Girardi, L., et al. 2012, *MNRAS*, 427, 127
 Brown, A. G. A., Dekker, G., & de Zeeuw, P. T. 1997, *MNRAS*, 285, 479
 Cantat-Gaudin, T., Mapelli, M., Balaguer-Núñez, L., et al. 2019, *A&A*, 621, A115
 Carpenter, J. M., Heyer, M. H., & Snell, R. L. 2000, *ApJS*, 130, 381
 Currie, T., Hernandez, J., Irwin, J., et al. 2010, *ApJS*, 186, 191
 Dame, T. M., Hartmann, D., & Thaddeus, P. 2001, *ApJ*, 547, 792
 Evans, D. W., Riello, M., De Angeli, F., et al. 2018, *A&A*, 616, A4
 Gaia Collaboration, Brown, A. G. A., Vallenari, A., et al. 2018, *A&A*, 616, A1
 Gaia Collaboration, Helmi, A., van Leeuwen, F., et al. 2018, *A&A*, 616, A12
 Gaia Collaboration, Prusti, T., de Bruijne, J. H. J., et al. 2016, *A&A*, 595, A1
 Gouliermis, D. A. 2018, *PASP*, 130, 072001
 Heyer, M. H., Brunt, C., Snell, R. L., et al. 1998, *ApJS*, 115, 241
 HI4PI Collaboration, Ben Bekhti, N., Flöer, L., et al. 2016, *A&A*, 594, A116
 Jose, J., Kim, J. S., Herczeg, G. J., et al. 2016, *ApJ*, 822, 49
 Kim, C.-G., & Ostriker, E. C. 2015, *ApJ*, 802, 99
 Koenig, X. P., Allen, L. E., Gutermuth, R. A., et al. 2008, *ApJ*, 688, 1142
 Kounkel, M., Covey, K., Suárez, G., et al. 2018, *AJ*, 156, 84
 Kuhn, M. A., Hillenbrand, L. A., Sills, A., Feigelson, E. D., & Getman, K. V. 2019, *ApJ*, 870, 32
 Lada, C. J., & Lada, E. A. 2003, *ARA&A*, 41, 57
 Lin, C. C., & Shu, F. H. 1964, *ApJ*, 140, 646
 Longmore, S. N., Kruijssen, J. M. D., Bastian, N., et al. 2014, in *Protostars and Planets VI*, ed. H. Beuther et al. (Tucson, AZ: Univ. Arizona Press), 291
 Mac Low, M.-M., McCray, R., & Norman, M. L. 1989, *ApJ*, 337, 141
 Pandey, A. K., Upadhyay, K., Ogura, K., et al. 2005, *MNRAS*, 358, 1290
 Román-Zúñiga, C. G., Ybarra, J. E., Megías, G. D., et al. 2015, *AJ*, 150, 80
 Sung, H., Bessell, M. S., Chun, M.-Y., et al. 2017, *ApJS*, 230, 3
 Tang, J., Bressan, A., Rosenfield, P., et al. 2014, *MNRAS*, 445, 4287
 Tapia, M., Costero, R., Echevarria, J., & Roth, M. 1991, *MNRAS*, 253, 649
 Taylor, M. B. 2005, in *ASP Conf. Ser. 347, Astronomical Data Analysis Software and Systems XIV*, ed. P. Shopbell et al. (San Francisco, CA: ASP), 29
 Tchernyshyov, K., Peek, J. E. G., & Zasowski, G. 2018, *AJ*, 156, 248
 Tenorio-Tagle, G. 1979, *A&A*, 71, 59
 Thornton, K., Gaudlitz, M., Janka, H.-T., & Steinmetz, M. 1998, *ApJ*, 500, 95
 Wright, N. J., & Mamajek, E. E. 2018, *MNRAS*, 476, 381
 Zasowski, G., Cohen, R. E., Chojnowski, S. D., et al. 2017, *AJ*, 154, 198